# Recellularization of Decellularized Allograft Scaffolds in Ovine Great Vessel Reconstructions

Ara Ketchedjian, MD, Alyce Linthurst Jones, MS, Paula Krueger, BS, Elliot Robinson, BS, Katrina Crouch, BS, Lloyd Wolfinbarger, Jr, PhD, and Richard Hopkins, MD

Department of Cardiothoracic Surgery and the Collis Cardiac Surgical Laboratory, Brown University and Rhode Island Hospital, Providence, Rhode Island, and LifeNet Tissue Services, Virginia Beach, Virginia

*Background.* Decellularized allograft tissues have been identified as a potential extracellular matrix (ECM) scaffold on which to base recellularized tissue-engineered vascular and valvular substitutes. Decreased antigenicity and the capacity to recellularize suggest that such constructs may have favorable durability. Detergent/enzyme decellularization methods remove cells and cellular debris while leaving intact structural protein "scaffolds." Allograft pulmonary artery tissues decellularized with an anionic detergent/enzyme methodology were tested in a long-term implantation model that used arterial wall repairs in the great vessels of juvenile sheep.

*Methods.* Twelve test sheep were implanted (n = 4) for each of three different scaffold protocols that compared traditional dimethylsulfoxide cryopreservation, cryopreservation followed by decellularization, and decellularization of fresh tissue. Four additional sheep served as controls (n = 2 sham, n = 2 fresh tissue). Patches were fashioned and implanted into pulmonary artery and aortic defects. Panel reactive antibodies (PRA) were mea-

sured over time (10 to 20 weeks). Explant histopathology determined recellularization morphology as well as calcium, collagen, and elastin distribution within explanted tissue.

*Results.* Unlike traditionally cryopreserved tissues, the decellularized tissues contained no residual cells or cellular debris before implantation, which correlated with measurable reductions in PRA. Decellularized explants demonstrated time-dependent migration of recipient cells through matrix, typically staining positive for $\alpha$-smooth muscle actin with no calcification.

*Conclusions.* The properties demonstrated seem consistent with characteristics necessary for implantable tissue-engineered scaffolds. The decellularization method described appears to create a biologically suitable ECM scaffold for in vivo migration of phenotypically appropriate cells while avoiding antigenicity and calcification.

(Ann Thorac Surg 2005;79:888–96)
© 2005 by The Society of Thoracic Surgeons

L imitations in growth and the reparative potential of current bioprosthetic valves and vascular reconstruction materials, as well as the acknowledged limited durability of cryopreserved allograft tissue, suggest a need for alternative substitute that would ideally recellularize in vivo, resulting in a structure analogous to native tissue [1, 2]. A tissue-engineered vascular scaffold that recellularizes appropriately has numerous theoretical advantages over nonviable materials including, but not limited to, the ability to grow, to repair itself, and to resist calcification. One approach to a tissue-engineered vascular scaffold is to decellularize allograft tissues.

Processing allograft tissues with detergents and enzymes may provide scaffolds that have the necessary biological and geometric recellularization potential [3]. Adequate decellularization should decrease antigenicity, avoid allosensitization, and remove cellular remnants that may serve as nidi for calcification and its associated consequences. Physical, metabolic, and synthetic charac-

teristics of migrating autologous cells (recellularization of acellular tissues) theoretically should provide the necessary structural and functional characteristics to sustain engineered tissue longevity and durability.

Various decellularization methodologies have been explored. Results have been mixed because cells and cellular debris remain and serve as nidi of calcification and may allosensitize the recipient [4, 5]. Such residua may promote increased innate and cellular immune responses, thus contributing to the failure of organized migration of phenotypically appropriate cells and compromising long-term remodeling of an acellular graft. Alternatively, robust thorough decellularization processes may degrade the physical characteristics of the matrix, leading to biomechanical and degenerative failure. These potentially adverse outcomes suggest the need to augment the in vitro assessment of acellular tissues with appropriate in vivo long-term testing and exposure to clinically relevant hemodynamic stresses.

Drs Wolfinbarger and Hopkins disclose that they hold patents in the general area of tissue-engineered heart valve technology.

A new strategy was devised to decellularize allograft matrices. This decellularization method utilizes an anionic detergent, recombinant endonuclease, and ion exchange resins to minimize processing reagent residuals in the tissues. The resulting acellular vascular scaffolds macroscopically appear similar to native tissue but are devoid of intact cells and contain virtually no residual cellular debris.

The primary hypothesis is that adequately decellularized tissues should avoid pronounced immune responses and nonspecific inflammation with consequential scarring and ultimately, mineralization, the avoidance of which allows for the migration and proliferation of phenotypically appropriate cardiovascular interstitial cells (ie, recellularization of the scaffold). To test our hypothesis, decellularized allograft tissues were used to reconstruct oval defects in pulmonary artery and aorta in a long-term ovine model. Physical and histologic evaluations of preimplant and postimplant tissues were performed to assay critical defining characteristics for the recellularization process that could determine structural and functional performance.

## Material and Methods

### Tissue Procurement and Dissection

Sheep tissues were obtained from Animal Technologies (Tyler, TX). Hearts were transported on wet ice in Roswell Park Memorial Institute (RPMI) 1640 medium supplemented with polymyxin B. Warm ischemic time was less than 3 hours, and cold ischemic time didn't exceed 24 hours. Twenty-four pulmonary conduits were dissected from the heart and truncated immediately distal to the leaflets. They were then placed in RPMI 1640 supplemented with polymyxin B, cefoxitin, lincomycin, and vancomycin at 4°C for 24 ± 2 hours. Representative 1 cm$^2$ tissue sections were placed in phosphate buffered water and vigorously vortexed, and 8 mL was injected into anaerobic and aerobic bottles (BacT/ALERT, bioMérieux, Marcy l'Etoile, France) and analyzed for 14 days for bacterial or fungal growth.

### Cryopreservation

Eight pulmonary trunks were cryopreserved according to standard clinical tissue bank practices in RPMI 1640 supplemented with 10% fetal calf serum and 10% dimethylsulfoxide. The temperature was reduced by 1°C/min until −40°C was achieved; then the pulmonary trucks were transferred to vapor phase liquid nitrogen (≤ −120°C) until used [2].

### Decellularization

After the thawing and removal of cryoprotectant from the tissues, previously cryopreserved conduit tissue was decellularized using a detergent/enzyme/water decellularization process developed at LifeNet (Virginia Beach, VA, US Patent 6,743,574). The grafts were placed in a decellularization flow-through chamber containing detergent (N-lauroyl sarcosinate [NLS]), enzyme (Benzonase, Novagen, Madison, WI), antibiotic (polymyxin B) solution,

and Tris buffer (decellularization solution). A peristaltic pump was used to circulate this solution through the tissue for 24 to 36 hours. After decellularization, the decellularization solution was drained from the system and sterile water was circulated through the tissue chamber and a cartridge of hydrophobic adsorbent resin and anion exchange resin beads for 24 to 36 hours. For decellularization of the eight "fresh" tissues, the sequence was identical except not preceded by cryopreservation.

### Detergent Residuals

Detergent residuals that remain in tissue after decellularization can be cytotoxic and inhibit cell adhesion, migration, and proliferation. A radiolabeled NLS detergent assay was conducted to validate that the described decellularization process resulted in tissues with minimal noncytotoxic detergent residuals. Tissue samples were decellularized in the presence of tritiated NLS at 1μCi per 64 μmol/mL according to normal protocol, then digested in 4 mL of 1N NaOH at 90°C for 4 hours, cooled, and vortexed. Aliquots (0.1mL) from this were added to liquid scintillation cocktail and the disintegrations per minute (DPMs) determined using a liquid scintillation counter. The protein concentration in each sample was determined using the Pierce bicinchoninic acid (BCA) protein assay (Rockford, IL). The DPMs were converted to total nanomoles of NLS and normalized using the total protein content of the samples. It was determined that there was greater than a 2-log reduction in the amount of NLS, indicating the detergent was reduced by the water/resin washout procedure to insignificant residual tissue levels.

### DNA Quantitation

Residual DNA was quantified after decellularization by using a Nucleon HT DNA extraction assay (Amersham Biosciences, Piscataway, NJ). Tissue samples (25 mg) were crushed over liquid nitrogen and digested with a detergent solution and proteinase K at 50°C for 3 hours. The DNA was separated from contaminating proteins and lipids by adding-* sodium perchlorate, chloroform and Nucleon resin (Amersham Biosciences). The extracted DNA was precipitated with cold ethanol, centrifuged into a pellet, and resuspended in buffer. PicoGreen dye (Molecular Probes, Eugene, OR) was added to the resuspended pellet and the extractable DNA quantified fluorometrically. The amount of extractable DNA was calculated per wet weight of tissue and expressed as a percent reduction in extractable DNA relative to nondecellularized tissues. All decellularized tissues used in this study had 99.8% or greater reduction in DNA content.

### Tissue Storage

The decellularized tissues were cryoconserved for storage at 4°C. Cryoconservation is the process of sublimating water from frozen tissue after it has been decellularized (LifeCell, Branchburg, NJ) (US Patent 5,336,616). The tissue was immersed in 75% maltodextrin for 24 hours and then frozen at −80°C. To sublimate the water, the

tissue was aseptically packaged and placed in a freeze dryer in which the temperature was lowered by 2°C/min to −45°C, pulling a vacuum to 3000 mT, and drying at −50°C.

### Thaw/Dilution and Rehydration of Cryoconserved Tissues

Before implant, the tissues were placed into a flow-through chamber and the cryoprotectant was serially diluted with Ringer's lactate solution (LifeNet, US Patents 6,326,188 and 5,879,876)

### Surgical Model

Twelve 30-kg juvenile sheep were used for patch reconstructions of great vessel defects. The juvenile sheep long-term implant model was chosen as it has been consistently recommended as the most relevant to human cardiovascular biological valve performance (ISO 5840:1996 and FDA Replacement Heart Valve Guidance Document: 1994). Animal handling was in accordance with guidelines from the Brown University Institutional Animal Care and Use Committee, which approved the experimental procedures. All studies conformed to the *Guide for the Care and Use of Laboratory Animals* (National Institutes of Health publication 85-23, revised 1985).

Anesthesia was induced with propofol (2 mg/kg.). Standard aseptic surgical techniques and cardiopulmonary bypass support were used. Each sheep received two patches (one descending aortic arch and one pulmonary artery) fashioned from one of the test material types (cryopreserved, cryopreserved/decellularized, or fresh decellularized). Surgical defects were created for implantation in the descending thoracic aorta and pulmonary artery. Elliptical patches of matching size were fashioned and sutured into the defects using 4-0 polydioxanone (Ethicon, Summerville, NJ). All animals received postoperative antibiotics (5 mg/kg amoxicillin and 5 mg/kg amikacin, twice daily) for 2 weeks and buprenorphine (1 amp twice daily) analgesia for 3 days.

Two sheep per test material were explanted at 10 weeks and another 2 sheep were explanted at 20 weeks Explantation was performed through the same thoracotomy incision. Once the patch length and width were measured under physiologic pressures, the animals were euthanized for tissue harvest by the administration of phenobarbital (324 mg/mL) 15 mL/100 pounds through peripheral intravenous access.

### Panel Reactive Antibodies Assay by Flow Cytometry

We have previously reported a modified panel reactive antibodies (PRA) assay useful for ovine implants [6]. In brief, serial blood samples were collected from the jugular vein. Serum was purified with a HiTrap purification system (Amersham Biosciences), and incubated with beads (One Lambda Inc, Canoga Park, CA) seeded with 30 major histocompatibility complex (MHC) class I and 30 MHC class II antigen isotypes for 30 minutes in the dark with continuous gentle shaking, washed with buffer solution, and centrifuged at 11,500 rpm for 2 minutes. Supernatant was removed and the beads were incubated with a rabbit

antisheep fluorescein isothiocyanate antibody (Jackson Immuno-Research, West Grove, PA) for 30 minutes (in the dark) with continuous shaking. The beads were washed with buffer solution and centrifuged at 11,500 rpm for 2 minutes. Supernatant was removed and the beads were fixed in 10% formalin and analyzed on a FACS flow cytometer (Becton Dickson, Franklin Lakes, NJ).

### Histology

Movat's pentachrome, hematoxylin and eosin (H&E) staining (Vector, Burlingame, CA) and alizarin staining were performed by standard histologic methods.

### MHC I and II Immunohistochemical Staining

Segments of preimplant tissue patches were flash frozen, stored at −80°C until sectioning, fixed with cold acetone, and stored at −20°C until staining. Slides were incubated in serum-free protein blocking solution (Dako, Carpinteria, CA) for 15 minutes at room temperature and rinsed in deionized water. Mouse antisheep MHC I and II primary antibodies (VMRD, Pullman, WA) were diluted 1:50 in 0.1 mol/L phosphate buffer with 5% fetal bovine serum. Slides were placed in primary antibody for 30 minutes. Slides were rinsed with deionized water and subsequently incubated with a secondary antibody, biotinylated mouse immunoglobulin G (Vector ABC [avidin-biotin complex], Vector Labs, Burlingame, CA) for 30 minutes. Slides were incubated in Vector diaminobenzidine (DAB) peroxidase substrate for 5 to 10 minutes to visualize the target antigen, then rinsed and stained with Vector Hematoxylin for 5 minutes, rinsed, dehydrated and CitriSolv fixed (Fisher Scientific, Pittsburgh, PA).

### Actin Immunohistochemical Staining

Explanted allograft materials were fixed in 10% phosphate buffered formalin, processed, and embedded in paraffin. Specimens were sectioned at 8 $\mu$m, and standard histologic techniques were used to prepare the slides. Endogenous peroxidases in the tissue were quenched using a 0.03% hydrogen peroxide solution in deionized water for 5 minutes at room temperature. Nonspecific protein binding was blocked using phosphate-buffered saline (PBS) with bovine serum albumin (BSA) (Ameresco, Solon, OH) plus 5% normal horse serum (NHS) for 30 minutes at room temperature. Mouse anti-$\alpha$-smooth muscle actin (Sigma, St. Louis, MO) was diluted 1:20,000 in PBS/BSA plus 5% NHS. Slides were rinsed in deionized water three times, and then incubated in Vector Nova Red peroxidase substrate for 5 to 10 minutes to visualize the target antigen. Slides were rinsed in deionized water three times for 5 minutes and stained using Vector Hematoxylin, Gill's formulation for 5 minutes, and then rinsed, dehydrated, and mounted.

### Statistical Analysis of Changes in Patch Dimensions

Dimensional areas are expressed in mm². Ratios for change in patch area were calculated by dividing the explant dimensional values by implant dimensional values. The mean of each subgroup was compared and

*Table 1. Dimensional Measurements of Implants and Explants*

| | Implant Dimensions mm | (Area) mm² | Explant Dimensions mm | (Area) mm² |
|---|---|---|---|---|
| **Patch Type: Aortic position at 10-weeks** | | | | |
| Cryopreserved | 17 × 10 | (133.4) | 22 × 12 | (207.0) |
| Cryopreserved | 28 × 22 | (438.5) | 25 × 22 | (431.7) |
| Fresh decell | 23 × 14 | (252.7) | 25 × 20 | (392.5) |
| Fresh decell | 25 × 18 | (353.2) | 28 × 20 | (439.6) |
| Cryo decell | 20 × 15 | (235.5) | 20 × 15 | (235.5) |
| Cryo decell | 15 × 14 | (164.8) | 16 × 14 | (175.8) |
| **Patch Type: Pulmonary position at 10-weeks** | | | | |
| Cryopreserved | 20 × 12 | (188.4) | 30 × 20 | (471.0) |
| Cryopreserved | 31 × 14 | (340.6) | 30 × 20 | (471.0) |
| Fresh decell | 30 × 19 | (447.4) | 32 × 22 | (552.6) |
| Fresh decell | 30 × 12 | (282.1) | 25 × 18 | (353.2) |
| Cryo decell | 29 × 20 | (455.3) | 30 × 25 | (588.7) |
| Cryo decell | 27 × 16 | (339.1) | 33 × 20 | (518.1) |
| **Patch Type: Aortic position at 20-weeks** | | | | |
| Cryopreserved | 30 × 20 | (471.0) | 30 × 40 | (942.0) |
| Cryopreserved | 25 × 20 | (392.0) | 25 × 33 | (647.0) |
| Fresh decell | 21 × 14 | (230.7) | 22 × 15 | (259.0) |
| Fresh decell | 25 × 15 | (294.3) | 30 × 25 | (588.7) |
| Cryo decell | 27 × 24 | (508.6) | 25 × 25 | (490.6) |
| Cryo decell | 20 × 14 | (219.8) | 18 × 10 | (141.5) |
| **Patch Type: Pulmonary position at 20-weeks** | | | | |
| Cryopreserved | 35 × 25 | (686.8) | 30 × 30 | (706.5) |
| Cryopreserved | 30 × 25 | (588.7) | 30 × 35 | (824.2) |
| Fresh decell | 30 × 20 | (471.0) | 34 × 30 | (471.0) |
| Fresh decell | 30 × 20 | (471.0) | 35 × 30 | (824.2) |
| Cryo decell | 35 × 25 | (686.8) | 35 × 25 | (686.1) |
| Cryo decell | 30 × 25 | (588.7) | 33 × 28 | (725.3) |

Table records patch dimensional measurements in millimeters (mm). Areas calculated as mm². When comparing explant/implant ratios there was no statistical difference between the means in each group by analysis of variance ($p = 0.4$ 10 wk aortic; $p = 0.2$ 10 wk pulmonary; $p = 0.2$ 20 wk aortic; $p = 0.8$ 20 wk pulmonary).

Area calculation is based on a formula for an ellipse (oval patches) so A = $\pi$ r$_A$r$_B$ where r$_A$ = ½ length (long axis of oval patch) = radius A;     and r$_B$ = ½ width (short axis of oval patch) = radius B.

Cryopreserved = traditional dimethylsulfoxide (DMSO) cryopreservation;     fresh decell = decellularization protocol using freshly harvested pulmonary artery wall tissue;     cryo decell = pulmonary artery wall cryopreserved with DMSO then thawed, rehydrated and subjected to decellularization protocol.

analyzed by analysis of variance (ANOVA) (SigmaStat, Version 2.03, Systat Software, Inc, Point Richmond, CA) using the Student-Newman-Keuls method with statistical significance determined at $p$ less than 0.05.

## Results

Pulmonary allograft patches were prepared for implant by three different methodologies: (1) classically cryopreserved (control) tissue, (2) cryopreserved, thawed, then decellularized tissue and (3) fresh, decellularized tissue. Tissues in groups 2 and 3 were cryoconserved for storage before implant. At explant surgery, all patches appeared to be nicely incorporated into the great vessel repairs without aneurysms or infection. Animals were sacrificed at the 10-week and 20-week designated postimplantation intervals.

Dimensional measurements were made at physiologic pressures during implants and explants (Table 1). There were no statistical differences in the explant/implant ratios for any of the patches treated by these protocols compared with the other groups at any time period or position ($p = 0.40$, 10 weeks aortic; $p = 0.29$, 10 weeks pulmonary; $p = 0.29$, 20 weeks aortic; $p = 0.80$, 20 weeks pulmonary; ANOVA).

Preimplant H&E staining revealed no intact cells or microscopically identifiable debris in either the cryopreserved/decellularized or the fresh/decellularized tissues (Fig 1). The classically cryopreserved control tissues demonstrated cellularity throughout (Fig 2). Immunohistochemistry staining for MHC I and II antigens revealed no intact cells and only very rare staining of residual cell debris (ie, negative in most high power [×200] fields) in the decellularized tissues compared with the grossly positive staining throughout in the classically cryopreserved patches.
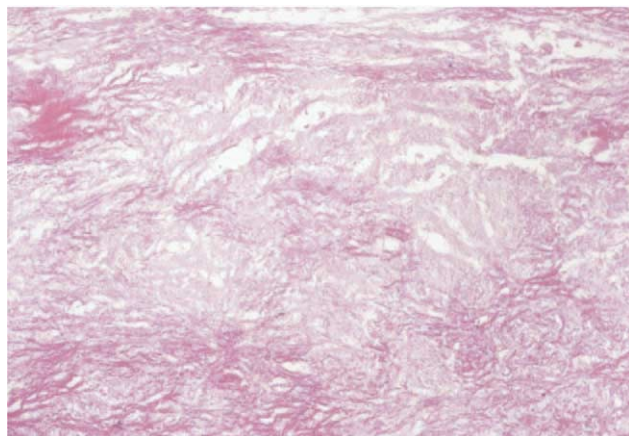
Fig 1. *Hematoxylin and eosin staining of preimplant decellularized tissue demonstrates no visible cells or debris (×200).*



Fig 2. *Hematoxylin and eosin staining of preimplant cryopreserved tissue demonstrates an abundance of cells throughout the matrix (×200).*

Histologic preparations of the explanted patch grafts stained with H&E and Movat's pentachrome demonstrated that classically cryopreserved tissues became acellular over time (Fig 3). They developed the fibrous sheathing typical for the histologic appearance documented in both animal and human cryopreserved allograft valve explants consisting of layers of fibroblast cells that line the luminal side and encapsulate the adventitial aspects, which may represent a classic foreign body response routinely seen in surgical implants of many types [2]. Both decellularized tissue types (cryopreserved/decellularized and fresh/decellularized) displayed time-dependent recellularization.

Ten-week explants of decellularized tissues demonstrated small numbers of infiltrating fibroblast-like cells in the pulmonary artery and descending thoracic aorta implant sites (Fig 4A). Twenty-week explants of decellularized tissues demonstrated cellularity throughout the matrix in the pulmonary artery and descending thoracic aorta implant sites (Fig 4B). Movat's pentachrome staining of the decellularized explants demonstrated cells infiltrating the elastin bands in a similar time-dependent fashion in the pulmonary artery and descending thoracic aorta implant sites (Fig 5A). $\alpha$-Smooth muscle actin immunohistochemistry staining suggested that most of these infiltrating interstitial cells were biologically active myofibroblasts (Fig 5B). Partial endothelialization along the luminal portion of the patch graft was seen in some sections. No differences could be discerned that distinguished between decellularized patches with or without preceding cryopreservation.

Alizarin staining demonstrated positive calcification in the classically cryopreserved patch explants (Fig 6A) after 10 and 20 weeks in both the pulmonary artery and descending thoracic aorta implantation sites. The cryopreserved/decellularized and fresh/decellularized patch explants were negative for calcification after 10 and 20 weeks in vivo except around sutures. The results were the same in both implantation sites (Fig 6B).
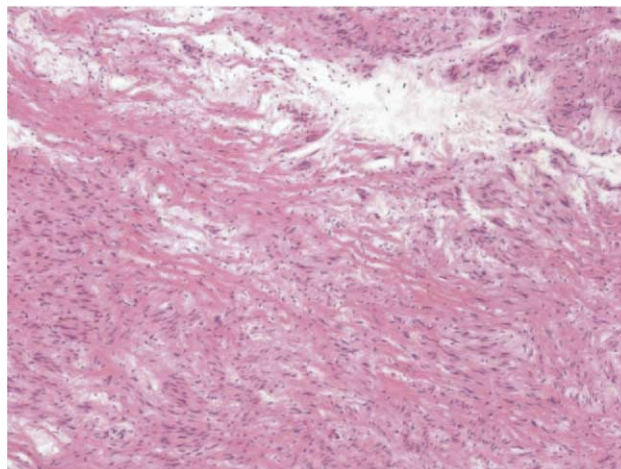
## Comment

Acellular tissues have been identified as a possible tissue-engineered solution for creating valvular and vascular tissue replacements. Infiltration of autologous, biologically active, phenotypically appropriate cells into an acellular collagen matrix could potentially provide reparative and functional advantages over current clinical nonviable prosthetics. If this recellularization process can occur in vivo, then perhaps preimplant bioreactor-based (cell seeding) recellularization methods may be unnecessary.

We compared traditionally cryopreserved ovine patches to cryopreserved ovine patches that were thawed and decellularized, as well as to ovine patches decellularized from "fresh" tissues. The patches were implanted into sites in the pulmonary and aortic circulation of
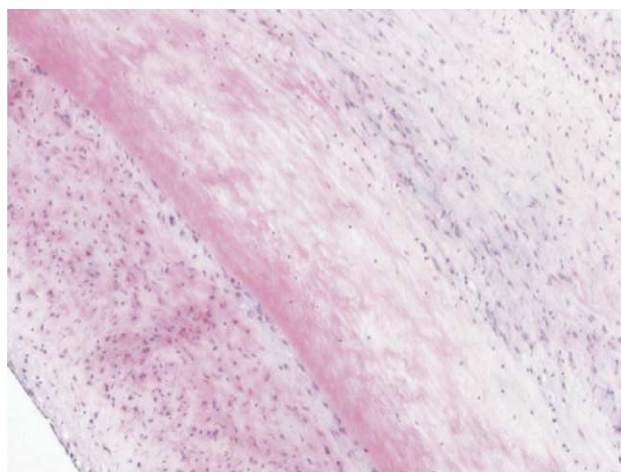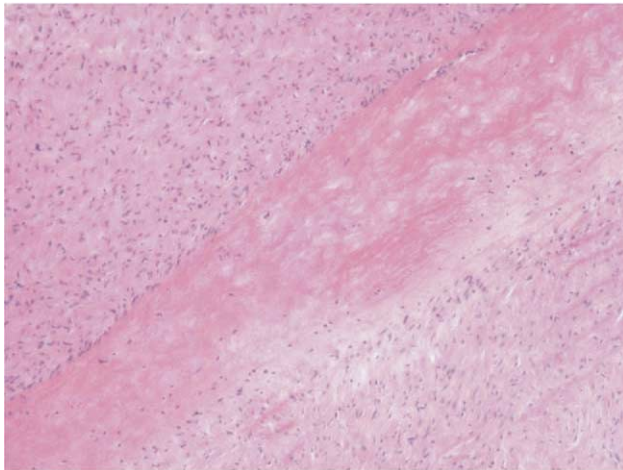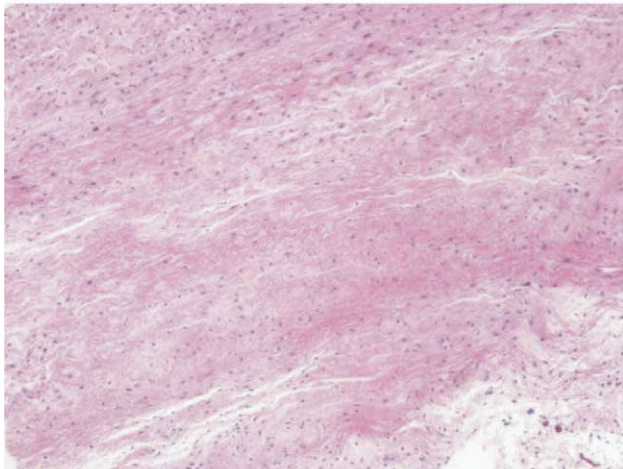


Fig 3. *Hematoxylin and eosin staining of cryopreserved tissue after 10 weeks of implantation in the pulmonary circulation of ovine model. There is fibrous sheathing of luminal and adventitial aspects, with a loss of cellularity within the matrix (×200).*
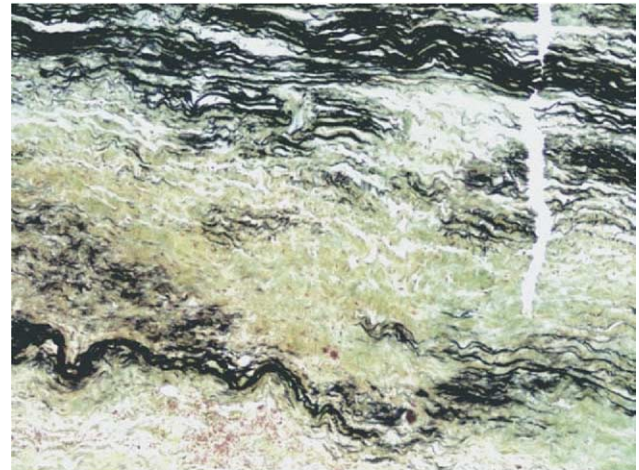
Fig 4. (A) Hematoxylin and eosin (H&E) staining of decellularized tissue after 10 weeks of implantation in the arterial circulation ovine model. Small amounts of cellular infiltration within the matrix are identified (×200). (B) H&E staining of decellularized tissue after 20 weeks of implantation in the arterial circulation of ovine model. Cellularity is identified throughout the matrix (×200).
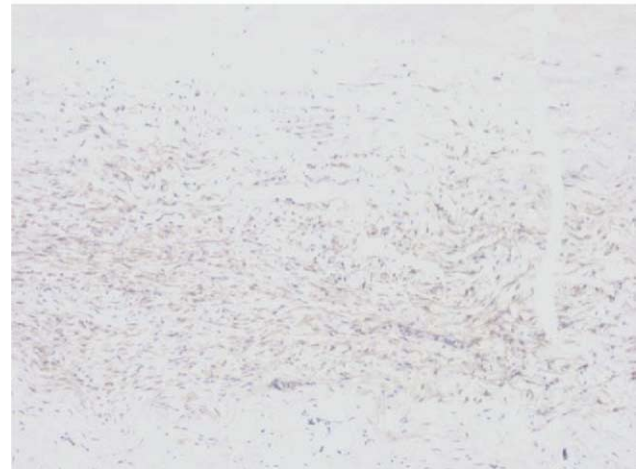


Fig 5. (A) Movat's staining of decellularized tissue after 20 weeks of implantation in the ovine model demonstrated cellular invasion within the elastin bands (×200). (B) Actin staining demonstrates that the infiltrating cells are migrating from the adventitial border and are biologically active for the synthesis of α-smooth muscle actin. Fissure artifact establishes orientation. Note minimal cell migration beyond the elastin bands (×200).

juvenile female sheep to evaluate structural performance and their ability to recellularize in vivo at 10 and 20 weeks.

The immunologic, histologic, physical, and functional data evaluated suggested that these allografts were potentially useful acellular scaffolds. The decellularized tissues did not seem to provoke immune rejection or calcification and were stable in the surgical reconstructions for the time period assessed. No aneurysmal changes were observed and no patches became infected. In addition, the decellularized matrices were infiltrated in vivo with autologous, seemingly phenotypically appropriate cells over the time course investigated, as evidenced by the H&E staining, Movat's pentachrome staining, and α-smooth muscle actin immunohistochemical staining.

Recellularization of decellularized tissues seemed to

occur in a time-dependent fashion. Ten-week explants demonstrated fibrous sheathing, which appears to be a significant step in the migration of cells, on both the adventitial and luminal aspects. The adventitial sheath has greater depth and contains more cells penetrating into the tissue than does the luminal sheath. The luminal sheath is more extensive in the aorta, which is likely secondary to the higher pressure experienced in this environment. Endothelialization of the sheath can occur. In addition, small numbers of cells were identified penetrating into the elastin bands of the implanted acellular matrix at 10 weeks. By 20 weeks, cells were seen throughout the matrix.

Observation of relative cell distributions demonstrated slower recellularization in the luminal side, suggesting that cells migrate into the matrix primarily from the

Fig 6. (A) Alizarin S staining of cryopreserved tissue demonstrated varying amounts of calcification. Calcification occurred at the suture lines as well as within the tissue matrix ($\times$200). (B) Alizarin S staining of decellularized tissue demonstrated calcification isolated to the suture lines. The tissue matrix was void of mineralization ($\times$100).

eration, and differentiation of tissue-appropriate cell types while still functioning effectively as a surgical implant to replicate the original native cardiovascular structure and function.

That the explant morphology suggested only patchy reendothelization is of significant interest because the cell composition of cardiovascular structures is heterogenous. The arterial walls contain endothelium, myofibroblasts, fibroblasts, smooth muscle cells, dendritic cells, and vascular structures in addition to the defined structural protein elements. Valve leaflets contain predominantly endothelium and myofibroblasts.

It is likely that a well-functioning endothelium requires an appropriate matrix cell population for communication, leading to cell and tissue functionality as well as providing appropriate triggers for cell population maintenance, migration, and proliferation. For example, the endothelium is likely responsible for being responsive to sheer stress and then "signals" the myofibroblast cell population to synthesize more structural protein such as collagen and elastin in response to the sheer stress or higher pressures. The situation is likely even more complex in that the contractile elements of the myofibroblast may be responsible for interpreting pressure stress, which is then also converted to signals for collagen production, smooth muscle migration, and endothelial cell proliferation. The developing field of cell signaling and cell–cell communication will help clarify these issues, but it is certainly likely that reendothelization of tissue-engineered vascular constructs will, in part, depend upon the restoration of an appropriate interstitial matrix cell population.

Classically cryopreserved allograft tissues such as xenograft bioprosthetics clinically demonstrate decreased durability over time, with specific failure modes particular to the processing methods [2]. Experimental and clinical data have implicated immune responses as contributing factors to the failure of cryopreserved allografts and xenograft bioprosthetics [2, 8–16]. Virtually all cryopreserved homografts demonstrate acellularity within a year of implantation [16, 17]. The lack of cells and cellular function limits tissue growth, performance, and reparative capacity; such "tissues" typically scar and then mineralize, which often leads to dysfunction.

Chronic rejection of cells in classically cryopreserved allograft tissues promotes the migration of inflammatory cells, exacerbating tissue degeneration, fibrosis, and functional failure. The cell repopulation of these decellularized scaffolds is unlike the typical fate of cryopreserved allografts that contain donor cells (as currently used clinically) in which such recellularization rarely occurs, perhaps as a consequence of the presence of necrotic cell debris or even apoptotic cells that block by specific cell signals the repopulation by autologous cells [2].

Or, perhaps the absence of allosensitization by vascular human leukocyte antigens may help avoid both humoral and cell-mediated chronic rejection [18, 19]. Such immune responses may prevent autologous recellularization. As we have previously reported, and supported by the data reported here, the anionic detergent/

adventitial aspect rather than the lumen and indicating that local cells, rather than circulating pluripotent progenitor cells, are the likely source of infiltrating myofibroblasts. Migrating fibroblast-like cells were found to stain positively for $\alpha$-smooth muscle actin, which is consistent with the dual phenotype of vascular and valve leaflet myofibroblasts [7]. This seems to indicate that a decellularized matrix can be conducive to autologous recellularization by phenotypically appropriate cells.

If autologous recellularization is not more complete or extensive with a longer implant interval (eg, 1 year), then the process of recellularization may need to be accelerated by preseeding the allograft scaffold with preselected cell lines that are either derived from the putative recipient or have been rendered nonantigenic within species. An alternative strategy would be to pretreat the scaffold with moieties designed to accelerate in-migration, prolif-

endonuclease decellularization method seems to result in protein scaffolds that minimize allosensitization [6]. Only 1 of 8 sheep that received tissues treated by either decellularization protocol demonstrated a positive elevation in PRA to MHC I, and none had PRA elevations for MHC II [6]. Classically cryopreserved tissues had variable responses (as also seen clinically), with two thirds of these animals demonstrating an elevation in PRA, especially to MHC class I antigens [6, 18]. That these ovine decellularized allograft tissues provoke minimal increases in PRA after implantation correlates well with the minimal amounts of residual MHC I and II antigens demonstrated in the preimplant tissue samples and demonstrates that a successful decellularization technology can result in tissue constructs that contain a minimal antigen load (within species) [5, 6, 18–23].

Decellularization of allograft tissue results in removal of cells and proteins, potentially creating defects, spaces, or voids within the collagen matrix that may lead to structural compromise [20]. To evaluate the structural and physical responses of decellularized tissues to the long-term exposure to physiologic pressure and sheer stresses, dimensional measurements were compared between implant and explant materials. There was no contraction or dilation of the decellularized tissues that would suggest an increased risk for catastrophic failure, such as rupture or calcification/fibrosis, compared with the cryopreserved control patch grafts. This suggests that the decellularization method described allows such tissue patches to retain sufficient mechanical strength for the vascular reconstructions tested, at least for the 20-week interval tested.

The interpretation of such data must be done with care. One interpretation is that these decellularized patches are effective because they are incorporated with salubrious wound healing without immune rejection and appear of sufficient strength and durability for the surgical applications tested. As such, these acellular scaffolds might be a superior choice compared with current inert manufactured options such as polytetrafluoroethylene or glutaraldehyde-treated bovine pericardium and are likely superior to classic but antigenic, cryopreserved homograft tissues. Decellularized allograft patches offer the advantage of favorable surgical conformational characteristics that suggests technical superiority for applications, such as neonatal and infant great vessel reconstructions, for which more rigid prosthetic materials are problematic.

Alternatively, these results could be described as autologous recellularization with in-migration of phenotypically appropriate matrix cells and formation of neointima, suggesting actual biological incorporation into the host matrix structure. These attributes may portend prolonged durability, resistance to prosthetic endocarditis, cell-mediated tissue repair, and protein renewal functions that approach the goals of tissue-engineered constructs but without preseeding or the need for extensive in vitro bioreactor manipulations.

As tested in a relevant juvenile sheep chronic implant model, this anionic detergent/recombinant endonuclease methodology seems to result in a tissue-engineered scaffold that maintains structural integrity, resists mineralization, and while avoiding allosensitization, tends to recellularize with phenotypically appropriate cells. Decellularized constructs such as the ones tested in these experiments may be fashioned from human tissues, including previously stored "viable" cryopreserved tissues. They may thus be clinically applicable to human nonvalve cardiovascular reconstructions such as infant pulmonary arterioplasties and neonatal hypoplastic aortic arch reconstructions. If the process is applicable to valve leaflets, valve conduit allografts could also potentially be "decellularized," with the intent of stimulating posttransplant cuspal and conduit wall recellularization.

The results also indicate that such decellularization technologies might be used to "reprocess" previously cryopreserved tissues that would otherwise be destroyed when storage time limits are exceeded, thus salvaging valuable tissue gifted for use in patients.

## References

1. Shinoka T, Ma PX, Shum-Tim D, et al. Tissue-engineered heart valves: autologous valve leaflet replacement study in a lamb model. Circulation 1996;94(9 Suppl):II164–8.
2. Hopkins RA. Cardiac Reconstructions with Allograft Tissues. New York: Springer-Verlag, 2004.
3. Steinhoff G, Stock U, Karim N, et al Tissue engineering of pulmonary heart valves on allogenic acellular matrix conduits: in vivo restoration of valve tissue. Circulation 2000;102(19 Suppl 3):III50–5.
4. Simon P, Kasimir MT, Seebacher G, et al. Early failure of the tissue engineered porcine heart valve Synergraft in pediatric patients. Eur J Card Thorac Surg 2003 23(6):1002–6.
5. Rieder E, Kasmir MT, Silberhumer G, et al. Decellularization protocols of porcine heart valves after implanting: efficiency of cell removal and susceptibility of the matrix to recellularization with human vascular cells. J Thorac Cardiovasc Surg 2004;127:399–405.
6. Ketchedjian A, Krueger P, Lukoff H, et al. Ovine panel reactive antibody assay of HLA responsivity to allograft bioengineered vascular scaffold. J Thorac Cardiovasc Surg 2004 [in press].

CARDIOVASCULAR

7. Messier RH, Bass BL, Aly HM. Dual structural and functional phenotypes of the porcine aortic valve interstitial characteristics of the leaflet myofibroblast. J Surg Res 1994;57:1–21.
8. Zhao X, Green M, Frazer IH, Hogan P, O'Brien MF. Donor-specific immune response after aortic valve allografting in the rat. Ann Thorac Surg 1994;57:1158–63.
9. Hoekstra F, Knoop C, Vaessen L, Wassenaar C, Borysewicz R, Weimar W. Donor specific immune response against human cardiac valve allografts. J Thorac Cardiovasc Surg 1996;112:281–6.
10. Hogan P, Duplock L, Green M, et al. Human aortic valve allografts elicit a donor-specific immune response. J Thorac Cardiovasc Surg 1996;112:1260–7.
11. Lupinetti FM, Cobb S, Kioschos HC, Thompson SA, Walters KS, Moore KC. Effect of immunological differences on rat aortic valve allograft calcification. J Card Surg 1992;7:65–70.
12. Hoekstra FM, Witvliet M, Knoop C. Donor-specific anti-human leukocyte antigen class I antibodies after implantation of cardiac valve allografts. J Heart Lung Transplant 1997;16:570–2.
13. Fischlein T, Schutz A, Haushofer M, et al. Immunologic reaction and viability of cryopreserved homografts. Ann Thorac Surg 1995;60(2 Suppl):S122–5.
14. Baskett RJ, Ross DB, Nanton MA, Murphy DA. Factors in the early failure of cryopreserved homograft pulmonary valves in children: preserved immunogenicity? J Thorac Cardiovasc Surg 1996;112:1170–9.
15. Dignan R, O'Brien M, Hogan P, et al. Aortic valve allograft structural deterioration is associated with a subset of antibodies to human leukocyte antigens. J Heart Valve Dis 2003;12:382–91.
16. Hilbert SL, Luna RE, Zhang J, et al. Allograft heart valves: the role of apoptosis-mediated cell loss. J Thorac Cardiovasc Surg 1999;117:454–62.
17. Koolbergen D, Hazekamp MG, de Heer E, et al. The pathology of fresh and cryopreserved heart valves: an analysis of forty explanted homograft valves. J Thorac Cardiovasc Surg 2002;124:689–97.
18. Hawkins JA, Lambert LM, Jones J. Immunogenicity of decellularized cryopreserved allografts in pediatric cardiac surgery: comparison with standard cryopreserved allografts. J Thorac Cardiovasc Surg 2003;26:247–52.
19. Christenson JT, Vala D, Sierra J, Beghetti M, Kalangos A. Blood group incompatibility and accelerated homograft fibroca1cifications. J Thorac Cardiovasc Surg 2004;127:242–50.
20. Hilbert SL, Yanagida R, Souza J, et al. Prototype anionic detergent technique used to decellularized allograft (homograft) valve conduits evaluated in the right ventricular outflow tract in sheep. J Heart Valve Dis 2004;13:831–40.
21. Vogt P, Stallmach T, Niederhauser U, et al. Explanted cryopreserved allografts: a morphological and immunohistochemical comparison between arterial allografts and allograft heart valves from infants and adults. Eur J Cardiothorac Surg 1999;15:639–45.
22. Allaire E, Bruneval P, Mandet C, Becquemin JP, Michel JB. The immunogenicity of the extracellular matrix in arterial xenografts. Surgery 1997;122:73–81.
23. Levy RJ, Schoen FJ, Howard SL. Mechanisms of calcification of porcine bioprosthetic aortic valve cusps: role of T-lymphocytes. Am J Cardiol 1983;52:629–31.

## INVITED COMMENTARY

This study describes another important attempt to overcome the limitations of currently available biomaterials in cardiac surgery. Decellularization of biomaterials, in this case ovine pulmonary patches, is thought to reduce antigenicity. However the efficiency of various protocols may differ importantly. In this study a combined anionic–enzymatic protocol is used and cells were effectively removed. Three groups of vascular patches, cryopreserved, cryopreserved–decellularized, and decellularized were implanted as vascular patches in the descending aorta and pulmonary artery in juvenile sheep for 10 and 20 weeks. The patches were well incorporated and no failures or calcification were observed. The antigenicity of decellularized samples appeared to be minimal as indicated by the absence of panel reactive antibodies. Cells repopulated the decellularized tissue samples in a time-dependent fashion and the staining for smooth-muscle actin suggested that these were myofibroblasts.

Several questions remain. The sheep was used as the standard model for the evaluation of heart valves, but it may not be the ideal model to transfer results to humans. Sheep have a tendency to endothelialize almost any material, whether biological or artificial. This is in sharp contrast to humans who seem to lack this ability. In fact, we have seen no cell repopulation of a decellularized heart valve implanted in humans up to 1.5 years. Furthermore, in this sheep model the cryopreserved samples behaved very differently from decellularized samples whether cryopreserved or not. It is well known that homografts become acellular after implantation, which in the case of this study corresponds to the cryopreserved allografts. What makes this acellular matrix so different from the decellularized material that it does not even become repopulated in sheep? Or in other words, what makes the decellularized matrix conducive to repopulation? The authors describe "fibrous sheathing of the tissues on the inside and more pronounced on the outside as part of the healing process" and suggest that this is important for the repopulation of the matrix. However, dense fibrous sheathing was an important failure mode leading to severe obstruction seen in the man implants with a decellularized heart valve.

As the pressure is mounting to develop superior biomaterials, especially in pediatric cardiac surgery where the need is particularly felt, we must remain cautious because experimental results may not be readily transferred to humans. The decellularized tissue may not be as biologically inert as is frequently suggested by removing the cells, but it may still elicit an inflammatory response.

*Paul Simon, MD*
*Marie-Theres Kasimir, MD*
*Erwin Rieder, MD*
*Guenter Weigel, MD*

*Department of Cardiac and Thoracic Surgery*
*Medical University of Vienna*
*Waehringer Guertel 18-20*
*Vienna, A-1090 Austria*
*e-mail: paul.simon@univie.ac.at*